Journal of Medicinal Chemistry

Article

pubs.acs.org/jmc

Mechanism Inspired Development of Rationally Designed Dihydrofolate Reductase Inhibitors as Anticancer Agents

Palwinder Singh,* Matinder Kaur, and Shaveta Sachdeva

Department of Chemistry, Guru Nanak Dev University, Amritsar-143005, India

Supporting Information

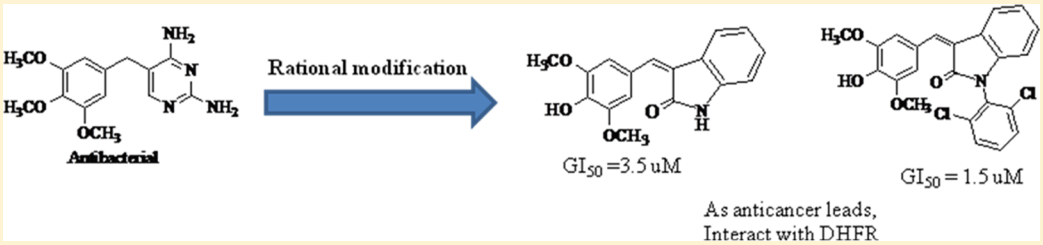

ABSTRACT: On the basis of structural analysis of dihydrofolate reductase (DHFR) (cocrystallized separately with NADPH, dihydrofolate and NADPH, trimethoprim), compounds **2** and **3** were optimized for inhibition of DHFR. Appreciable tumor growth inhibitory activities of compounds **2** and **3** over 60 human tumor cell lines were recorded. Combination of syringaldehyde and indole moieties in these two compounds was rationalized by the synthesis of compounds **4**−**7**, **10**, and **11**, which were found to have less tumor growth inhibitory activities than compounds **2** and **3**. Further, UV−vis and NMR spectral investigations showed significant interactions of compounds **2** and **3** with DHFR and inhibition of its catalytic activity was observed in the presence of these compounds. Therefore, modification of trimethoprim, an antibacterial drug with no tumor growth inhibition, led to the development of compounds **2** and **3** having appreciable anticancer activities that seem to be due to inhibition of DHFR.

INTRODUCTION

Dihydrofolate reductase (DHFR) is a ubiquitous enzyme showing its presence in protists as well as in plants and animals. The role of DHFR in folate metabolic pathway for biosynthesis of thymidine (precursor for DNA replication) is well established where it is responsible for reduction of dihydrofolate to tetrahydrofolate with the help of NADPH.[1] With it being responsible for generating raw materials of DNA replication, inhibition of DHFR forms the basis for treatment of various infectious diseases and is the target of antibacterial drugs like trimethoprim[2,3] as well as anticancer drugs 5-fluorouracil[4,5] and methotrexate.[6−8] Structural analysis of DHFR cocrystallized with NADPH, dihydrofolate, and trimethoprim provides an insight of the mode of interactions between DHFR and its cofactor, substrate, and inhibitor, respectively, which laid the basis for the design of new molecules as strategic inhibitors of DHFR metabolic pathway for chemotherapy of various diseases. As cofactor, NADPH is held by DHFR through H-bond interactions of the phosphate group with Ser64 (2.71 and 2.71 Å) amino acid of DHFR.[9−11] Oxygen atoms of linker phosphate also exhibit H-bond interaction with Thr96 and Gln95 at distances of 2.51, 3.26, and 3.08 Å, while amidic oxygen of nicotine unit is H-bonded to Ala7 (Figure 1). During the metabolic phase, dihydrofolate, the substrate of DHFR, is held in the substrate binding pocket of enzyme through ion pair formations between Arg57 and the COOH group (2.72, 3.09, and 2.80 Å) on one side and Asp27, NH_2, and N-5 of folate on the other end (Figure 1). The NH_2 group of folate also interacts with Thr111 through H-bond from a distance of 3.41 Å. Any alteration in the binding mode of NADPH/folate with DHFR led to changes in the folate metabolic pathway, which actually is the goal of DHFR inhibitors. The binding pattern of trimethoprim (TMP) with DHFR indicates that its trimethoxybenzene part is placed favorably in the hydrophobic pocket constituted by Phe92, Ile50, Val31, Leu28, and Trp22 (gray amino acids, Figure 2), while the pyrimidine part interacts through H-bonding with Asp27 (which otherwise forms ion pair with folate) and Thr111 and hence acts through the folate analogue inhibitor of DHFR.

Besides the development of a number of DHFR inhibitors[12−19] but medicinal use of a few of them,[2,8,20,21] where they also face the problem of drug resistance, there is continuous search for new chemical entities with potential of targeting of this enzyme. In the present investigation, a combination of ligand based and target structure based strategies were involved for the development of new molecules. Since folate is extended from Arg57 into the lower part to Thr111, Asp27 in the upper part, it was envisaged that a slight increase in the size of the inhibitor might make it interact with more amino acid residues, otherwise occupied by folate, and hence enhance efficacy of the inhibitor. Therefore, out of the two equally potent fragments of TMP (viz. trimethoxybenzene and pyrimidine (interacting with DHFR through hydrophobic

Received: March 17, 2012
Published: June 26, 2012

dx.doi.org/10.1021/jm300644g | J. Med. Chem. 2012, 55, 6381−6390

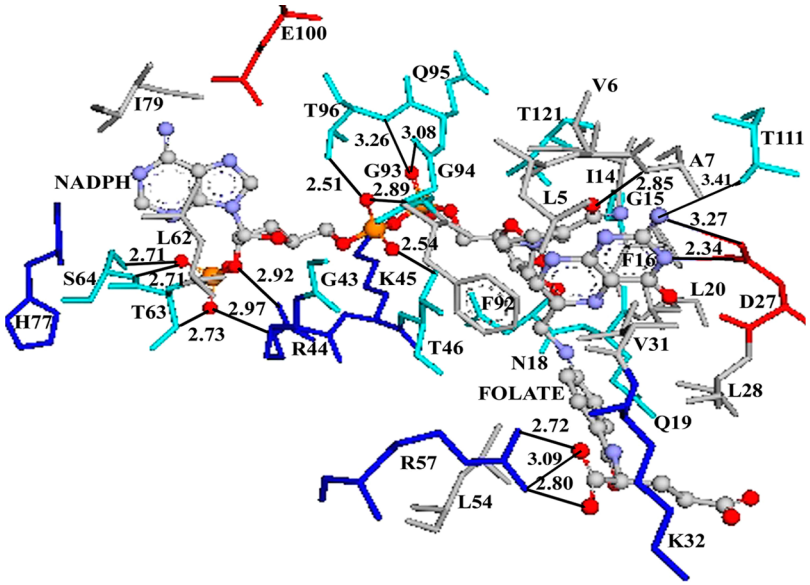

Figure 1. Crystal coordinates of DHFR cocrystallized with NADPH and folate (PDB entry 3FRD). Black lines indicate H-bonds with distances in Å. Purple, light blue, and gray colors correspond to positively charged, hydrophilic, and hydrophobic amino acids, respectively.

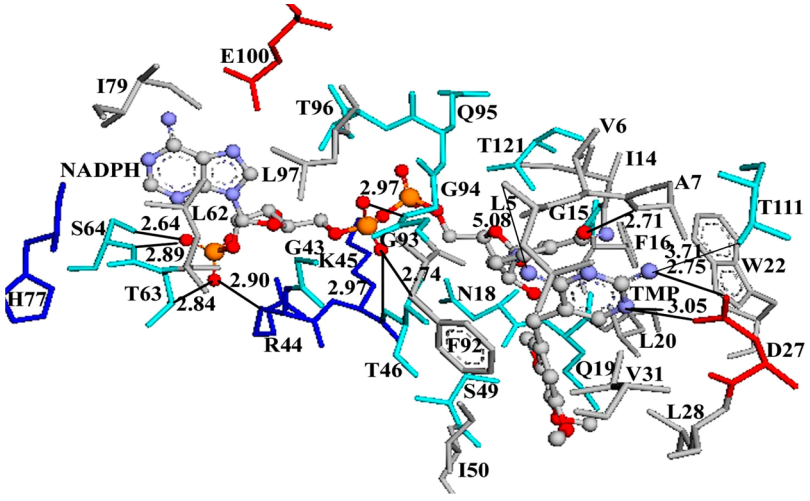

Figure 2. Crystal coordinates of DHFR cocrystallized with NADPH and TMP (PDB entry 2W9G). Black lines indicate H-bonds with distances in Å. Purple, light blue, and gray colors correspond to positively charged, hydrophilic, and hydrophobic amino acids, respectively.

and H-bond interactions, respectively)), it was planned to modify its one unit. The liver toxicity of TMP, associated with its conversion to pyrimidine iminoquinone methide through oxidation by human neutrophils,[22] made us modify the pyrimidine unit, and hence, in continuation of our efforts for developing safe, effective, and economical new chemotherapeutic agents using the indole moiety, two new molecules (**2**, **3**; Chart 1) were designed and screened for tumor growth inhibitory activities. Both the 2,6-dimethoxyphenolic component (part of trimethoprim metabolite, Chart 1) and indole moiety (biologically relevant moiety in place of pyrimidine of trimethoprim) of compounds **2** and **3** were considered as safeguards for their nontoxicity to biological systems.

Chart 1. Design of Molecules

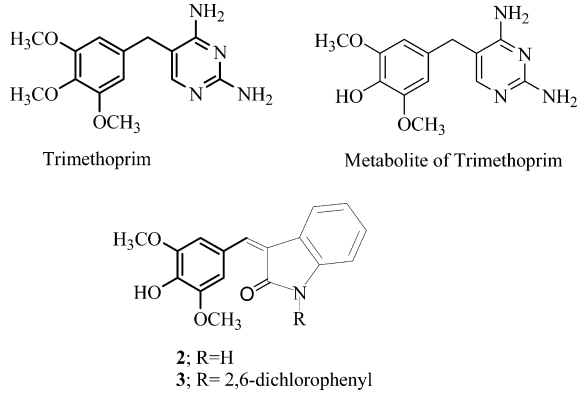

RESULTS AND DISCUSSION

Chemistry and Biology. Compounds **2** and **3** were built in quantitative yield by Knoevenagel condensation between an equimolar mixture of oxindole/indolinone and syringaldehyde (**1**) on irradiation under microwaves for 2−3 min (Scheme 1).

In vitro tumor growth inhibitory activities of both compounds were investigated on a 60 cell line panel of human cancer cells at five concentrations: 10^{-4}, 10^{-5}, 10^{-6},

dx.doi.org/10.1021/jm300644g | J. Med. Chem. 2012, 55, 6381−6390

Scheme 1. Synthesis of Compounds 2 and 3

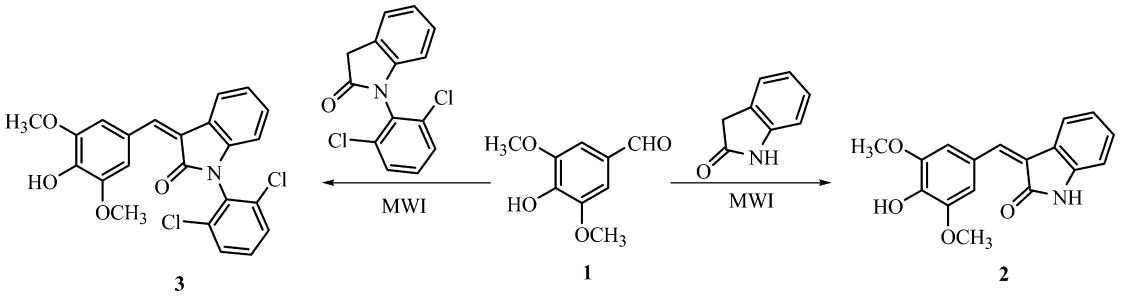

10^{-7}, and 10^{-8} M. Detailed results of these investigations in terms of GI_{50} (50% growth inhibitory concentration), TGI (total tumor growth inhibitory concentration), LC_{50} (50% lethal concentration), and therapeutic indices[23] over all the cancer cell lines are given in Table S1 (Supporting Information). Average GI_{50} values (over all the 60 cancer cell lines) of compounds **2** and **3** (Table 1) were 3.5 and 1.5 μM,

Table 1. Average GI_{50} (μM), TGI (μM), LC_{50} (μM) over 60 Cancer Cell Lines and Therapeutic Indices (TI) for Compounds 2 and 3, 6, 7, 11, and 12

compd	GI_{50}	TGI	LC_{50}	TI
2	3.5	21.4	72.4	20.6
3	1.5	19.4	61.6	41.1
6	3.9	17.7	50.1	12.8
7	2.0	9.1	27.5	13.7
11	5.5	16.9	47.8	18.4
12	1.8	3.2	9.1	5.1
indomethacin	64.3			
trimethoprim	no tumor growth inhibition at 10^{-5} M			

respectively, which were much better than those of indomethacin (GI_{50} = 64.3 μM)[24] and trimethoprim,[25] drugs carrying one of the two fragments (indole/syringaldehyde) present in compounds **2** and **3**. Compound **2** also showed specificity for certain cell lines like SR, NCI-H522, UACC-257, OVCAR-3, A498, MCF7, HS 578T, and MDA-MB-468 with GI_{50} in the range 0.6–2.0 μM (Table S1). Compound **3** exhibited specificity for leukemia, colon, CNS, melanoma, ovarian, and prostate cancer cell lines with GI_{50} in the range 0.08–1 μM (Table S1). Total growth inhibitory concentration and LC_{50} were, respectively, 21.4 and 19.4 for compound **2** and 72.4 and 61.6 for compound **3**. The therapeutic indices of 20.6 and 41.1 for compounds **2** and **3**, respectively, were very much in line with that required for anticancer drugs. Therefore, modification of trimethoprim in the form of compounds **2** and **3** resulted in several-fold increase in tumor growth inhibitory activities of new compounds in comparison to that of trimethoprim, and ligand/target based design of new molecules was justified. Physicochemical parameters of compounds **2** and **3** also obey Lipinski's rule of 5, favoring their druglike properties (Table 2).

Table 2. Lipinski Values for Compounds 2 and 3

compd	log *P*	TPSA (Å^2)	n_{ON}	n_{OHNH}
2	2.76	60.56	6	1
3	5.78	49.71	5	0

The design and appreciable tumor growth inhibitory activities of compounds **2** and **3** led us to check experimentally the interactions of these compounds with DHFR and also to rationalize the combination of indole and syringaldehyde in compounds **2** and **3**. For this purpose, UV–vis and NMR spectral techniques were taken into consideration along with synthesis and anticancer activities of more compounds.

UV–Visible Spectral Studies of Interactions of Compounds 2 and 3 with DHFR. A solution of DHFR in HEPES buffer (10^{-3} M) at pH 7.2 exhibited UV–vis absorption bands at 218 and 269 nm (red trace, Figure 3).

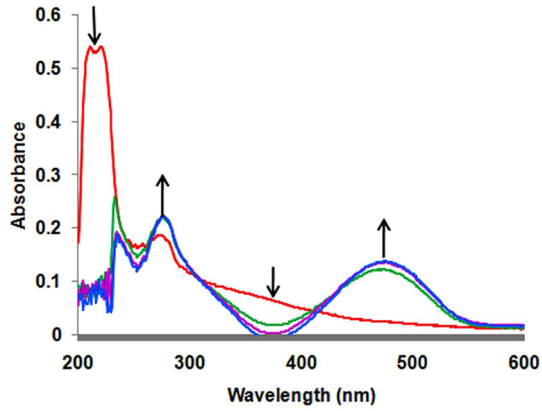

Figure 3. Absorption spectra of dihydrofolate reductase (red trace) in the presence of increasing concentration of compound **2** (10^{-5} M). Arrows denote change in absorption with increasing concentration of compound **2**.

Stepwise addition of compound **2** (10^{-5} M, 10–40 μL) to the solution of DHFR resulted in a decrease of absorption intensity at 218 nm with an increase in absorption intensity at 269 nm and appearance of a new band at 478 nm. Alternatively, incremental addition of DHFR (5–30 μL) to solution of compound **2** in HEPES buffer at pH 7.2 resulted in a decrease in absorption bands at 260 and 375 nm (two absorption maxima of compound **2**) with the formation of a new band at 478 nm (Figure 4).

Similarly, stepwise addition of compound **3** (10^{-5} M, 10–40 μL) to a solution of DHFR in HEPES buffer (10^{-3} M) at pH 7.2 changed the absorption bands at 218 and 269 nm (Figure 5). Addition of DHFR (5–30 μL) to solution of compound **3** (10^{-5} M) (purple trace, Figure 5) resulted in a decrease in absorption intensity at 218, 269, and 375 nm (Figure 5). Binding constants of 2-DHFR and 3-DHFR were calculated as 1.3×10^7 and 1.6×10^7 M^{-1}, respectively (Table S4). Therefore, a change in UV–vis spectra of compounds **2** and **3** in the presence of DHFR clearly indicated their interactions

dx.doi.org/10.1021/jm300644g | J. Med. Chem. 2012, 55, 6381–6390

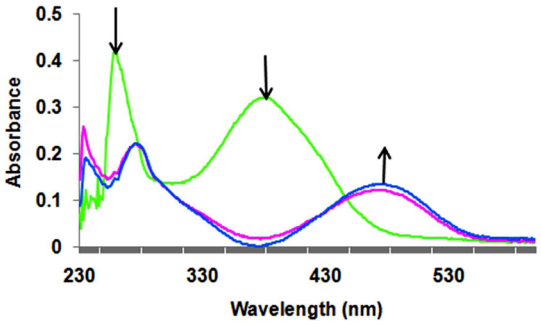

Figure 4. Absorption spectra of compound **2** (10^{-5} M, green trace) in the presence of increasing concentration of DHFR (5−30 μL). Arrows denote change in absorption with increasing concentration of DHFR.

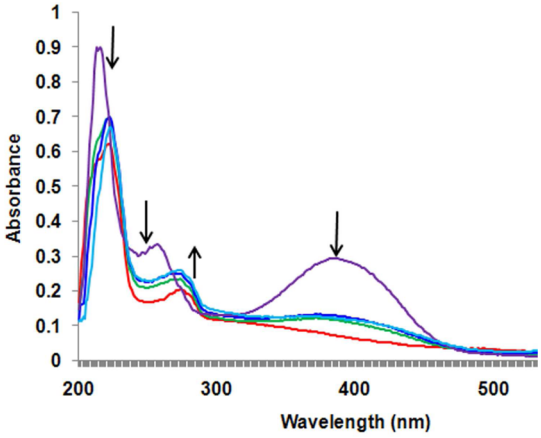

Figure 5. Absorption spectra of dihydrofolate reductase (red trace) and compound **3** (purple trace). Absorption spectrum of DHFR (red trace) changed to green trace on addition of compound **3**, while absorption spectrum of compound **3** (purple trace) changed to blue trace on addition of DHFR.

with DHFR. In order to check the possibilities that tumor growth inhibitory activities of compounds **2** and **3** might be due to inhibition of other enzymes, their interactions with thymidylate synthase (TS) and thymidylate phosphorylase (TP) (other enzymes involved in cancer propagation) were also studied. No change in UV−vis spectra of compounds on addition of TS and TP indicated noninteractions of compounds **2** and **3** with these enzymes. Molecular docking of compounds **2** and **3** in the active site of DHFR (PDB entries 3FRD and 2W9G) indicated H-bond interactions between compound and amino acid residues (Figures S15−S18, Supporting Information).

Effectiveness of Indole−Syringaldehyde Combination. As already mentioned, anticancer activities of compounds **2** and **3** were much improved over that of TMP. The effectiveness of indole and syringaldehyde combination in compounds **2** and **3** toward tumor growth inhibitory activities was further rationalized by the synthesis of other related compounds. By replacement of the indole moiety of compounds **2** and **3** with pyrimidine and pyrazole, compounds **4** and **5** were synthesized through the reaction of syringaldehyde with 2-(3-chlorophenyl)-5-methyl-2,4-dihydropyrazol-3-one and barbituric acid, respectively (Scheme 2).

Anticancer screening of compounds **4** and **5** over 60 human tumor cell lines showed very poor inhibition of tumor growth in the presence of these compounds, indicating the significant role of the indole moiety for anticancer activities of compounds **2** and **3**. Moreover, compounds **4** and **5** did not show interaction with DHFR, as indicated from UV−vis spectral investigations.

In order to replace the syringaldehyde component of compounds **2** and **3**, compounds **6** and **7** were synthesized through the reaction of 5-bromoindole-3-carboxaldehyde with 2-(3-chlorophenyl)-5-methyl-2,4-dihydropyrazol-3-one and reaction of indolinone with pyridine-2-carboxaldehyde, respectively, under MWI (Scheme 3).

Scheme 3. Synthesis of Compounds 6 and 7

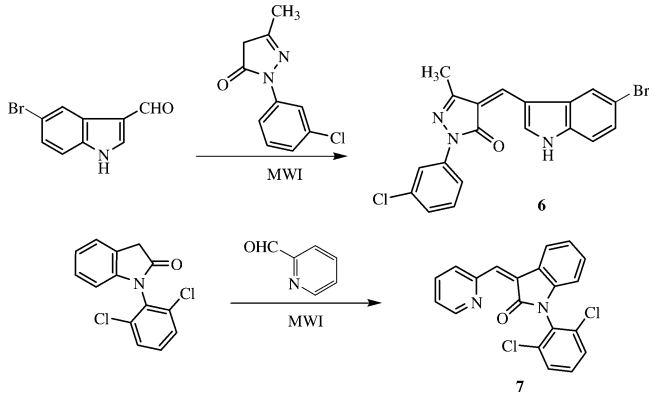

Anticancer screening of compounds **6** and **7** showed tumor growth inhibitory activities of these compounds (Table S2) with average GI_{50} values over all 60 tumor cell lines of 3.9 and 2.0 μM, respectively (Table 1), which are slightly higher than those of compounds **2** and **3**, indicating lower efficacy of compounds **6** and **7**. TGI, LC_{50}, and TI of compound **6** were recorded as 50.1 μM, 17.7 μM, and 12.8, respectively, while respective values for compound **7** were 9.1, 27.5, and 13.7 μM. UV−vis spectral based investigations showed a small change in

Scheme 2. Synthesis of Compounds 4 and 5

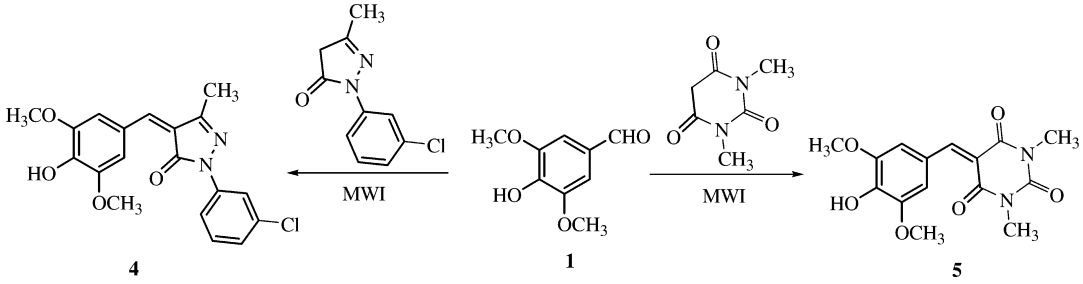

dx.doi.org/10.1021/jm300644g | J. Med. Chem. 2012, 55, 6381−6390

Scheme 4. Synthesis of Compounds 11 and 12

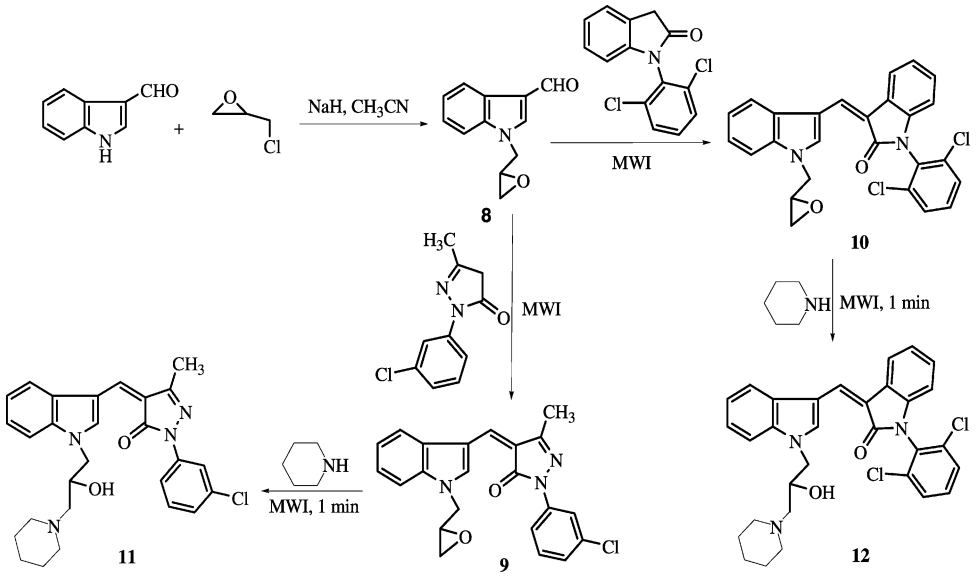

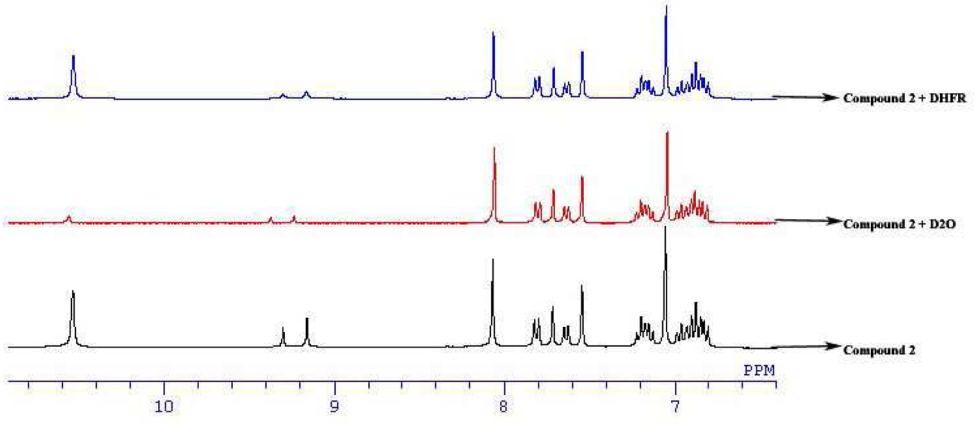

Figure 6. Part of ^{1}H NMR spectrum of compound **2** (lower trace). D_2O exchange (middle trace) showing exchangeable proton NH at δ 9.2 and 9.3 and exchangeable proton OH at 10.6. Compound **2** in the presence of DHFR (upper trace). Intensities of NH signals get decreased.

UV−vis spectra of compounds **6** and **7** on addition of DHFR, pointing toward poor interactions of these compounds with the enzyme (Supporting Information).

Further, the substitution at N-1 of indole of unbrominated compound **6** and a similar combination with indolinone provided compounds **11** and **12** (Scheme 4), which showed tumor growth inhibitory activities with average GI_{50} over all the tumor cell lines of 5.5 and 1.8 μM, respectively (Table 1). However, their respective TI (18.4 and 5.1) was poor compared to that of compounds **2** and **3**. These compounds showed specificity for certain cell lines like COLO 205, HCT-116, and SW-620 of colon cancer; M14 and SK-MEL-28 of melanoma; and CAK-1 and UO-31 of renal cancer by compound **11** with GI_{50} in the range 1.7−1.8 μM; while compound **12** inhibited tumor growth of almost all 60 cell lines at 1.3−2.0 μM (Table S3). Changes in UV−vis spectra of compounds **11** and **12** on addition of DHFR were also less than those observed for compounds **2** and **3** and were comparable to those of compounds **6** and **7** (Table S4).

Therefore, comparison of tumor growth inhibitory activities and UV−vis spectral studies (in the presence of DHFR) of compounds **2** and **3** with compounds **4**−**7**, **11**, and **12** clearly supported the combination of indole and syringaldehyde in compounds **2** and **3** for appreciable anticancer activities and interactions with DHFR.

^{1}H NMR Spectral Investigations. To further support the above experimental results and locate the site(s) of interaction(s) of compound with DHFR, ^{1}H NMR spectral investigations were performed. ^{1}H NMR spectra of **2** (48 mM), **3** (32 mM), and DHFR (6 μL) were recorded in 0.7 mL of DMSO-d_6 at 25 °C. In the ^{1}H NMR spectrum of compound **2** (lower trace, Figure 6), signals at δ 9.2, 9.3, and 10.6 correspond to exchangeable protons (NH, OH) as confirmed by their D_2O exchange (middle trace, Figure 6). Comparison of the ^{1}H NMR spectrum of compound **2** with the spectra of compounds **3** and **4** resulted in the assignment of signals at δ 9.2, 9.3 to NH and the assignment of the signal at δ 10.6 to OH of compound **2**. Addition of **6** μL of DHFR to solution of compound **2** in DMSO-d_6 resulted in a significant decrease in intensity of NH signals (δ 9.2, 9.3) of compound **2** (upper trace, Figure 6) while no change in OH signal was observed indicating interactions from NH of compound **2** with amino acid residues of DHFR.

dx.doi.org/10.1021/jm300644g | J. Med. Chem. 2012, 55, 6381−6390

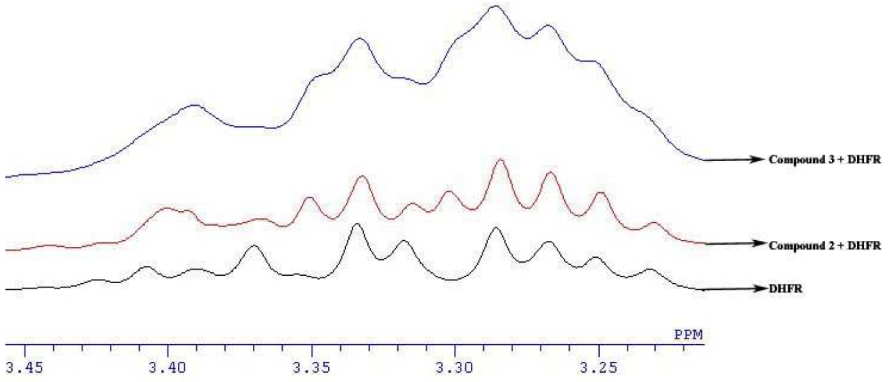

Figure 7. Part of ^{1}H NMR spectrum of DHFR (6 μL in 0.7 mL of DMSO-d_6) (lower trace). Change in resonances in the presence of compound **2** (middle trace) and compound **3** (upper trace).

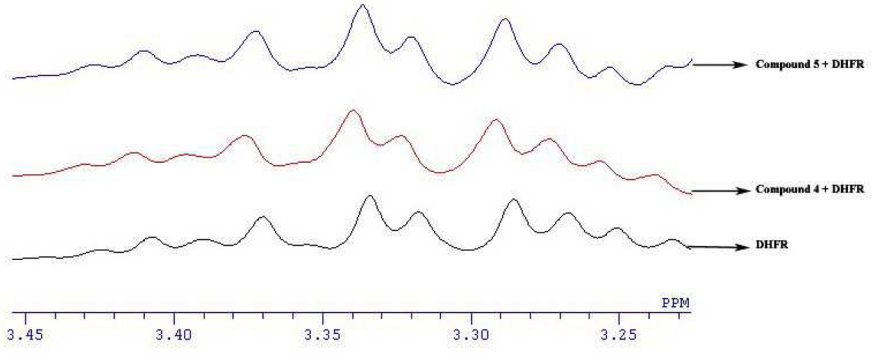

Figure 8. Part of ^{1}H NMR spectrum of DHFR (lower trace) and in the presence of compound **4** (middle trace) and in the presence of compound **5** (upper trace), indicating no change in ^{1}H NMR spectra of DHFR in the presence of compounds **4** and **5**.

A change in chemical shift and linewidth of some of the peaks of DHFR in the region 3−4 ppm (the region most distinctively visible in ^{1}H NMR spectrum of DHFR) (red trace, Figure 7) also indicated interactions of compound **2** and the enzyme.

Addition of 6 μL of DHFR to solution of compound **3** in DMSO-d_6 has also made changes in chemical shift and linewidth of DHFR signals in the region 3−4 ppm (blue trace, Figure 7). ^{1}H NMR spectra of a mixture of DHFR with compound **4** as well as with compound **5** did not exhibit any change either in the spectrum of DHFR or compounds (Figure 8). There is no interference of resonances from compounds in the region 3−4 ppm (^{1}H NMR spectra of compounds in Supporting Information).

Compounds **6**, **7**, **11**, and **12** also made changes in the ^{1}H NMR spectrum of DHFR (Figures 13 and 14 of Supporting Information). Hence, results of NMR spectral investigations are in parallel with those from UV−vis studies supporting significant interactions of compounds **2** and **3** with DHFR.

Dihydrofolate Reductase Inhibition Assay. The results of UV−vis and NMR based spectral investigations showing appreciable interactions between compounds **2**/**3** and DHFR prompted us to check the inhibition of DHFR activity by these compounds. Dihydrofolate reductase inhibition assay kit involving the DHFR mediated conversion of dihydrofolate to tetrahydrofolate in the presence of NADPH was used to investigate the inhibition of DHFR in the presence of compounds. It was observed that these compounds resulted in 80−90% inhibition in the enzyme activity at micromolar concentrations (Table 3).

Table 3. 80% Inhibitory Concentration (IC_{80}) of Compounds 2−7, 11, and 12 for DHFR

compd	IC_{80} (μM)
2	1.36[a]
3	10.05
4	
5	
6	
7	
11	1.06
12	0.89
methotrexate	1.44

[a]IC_{90}: compound **2** exhibited >90% inhibition at all five concentrations.

DHFR inhibitory activity of compounds **2**, **11**, and **12** was comparable to that of methotrexate, while compound **3** exhibited comparatively less inhibition of DHFR activity as evident from its IC_{80} value. Therefore, the results of the DHFR inhibition assay confirmed the UV−vis/NMR spectral results of interactions between compounds **2**, **3**, **11**, and **12** with DHFR. However, in the present assay, the effect of compounds **4**, **5**, **6**, and **7** on DHFR inhibition could not be studied, which might be because of their no interactions or fewer interactions with DHFR.

■ CONCLUSIONS

Structural analysis of dihydrofolate reductase in the presence of its cofactor, substrate, and inhibitor led to the design of new

molecules having structural similarities with the known antibacterial drug trimethoprim. A simple synthetic methodology that could be scaled up to procure tons of compounds was employed for the synthesis of the compounds. Compounds **2** and **3** showed significant tumor growth inhibitory activities over 60 human tumor cell lines and exhibited appreciable interactions with DHFR, as evidenced by UV−vis and NMR spectral studies. Compounds **2** and **3** also exhibited significant inhibition of DHFR activity with IC_{80} in the micromolar range, indicating DHFR inhibition as the probable mode of action of these compounds. Overall, a rational modification of the trimethoprim drug with no anticancer activity led to the development of two new molecules showing appreciable anticancer activities and interactions with DHFR.

EXPERIMENTAL SECTION

Chemical Synthesis. *General Remarks.* Melting points were determined in capillaries and are uncorrected. ^1H and ^{13}C NMR spectra were recorded on JEOL 300 and 75 MHz NMR spectrometers, respectively, using $CDCl_3$ and/or DMSO-d_6 as solvent. Chemical shifts are given in ppm with TMS as an internal reference. *J* values are given in hertz. Signals are abbreviated as follows: singlet, s; doublet, d; double−doublet, dd; triplet, t; multiplet, m. In ^{13}C NMR spectral data, +ve and −ve terms correspond to CH_3, CH, CH_2 signals in DEPT-135 NMR spectra. Chromatography was performed with silica 100−200 mesh, and reactions were monitored by thin layer chromatography (TLC) with silica plates coated with silica gel HF-254. Elemental analysis was performed on a Thermoelectron FLASH EA1112 CHN analyzer. Reactions under microwaves were performed using a microwave oven (INALSA model 1MW17EG) with microwave power of 700 W and operating frequency of 2450 MHz. IR and UV spectral data were recorded on FTIR 8400S Shimadzu and BioTek PowerWave XS instruments, respectively.

General Procedure for the Synthesis of New Conjugates. A finely ground mixture of aldehyde (1 mmol) and heterocycle based active methylene component (indolinone, oxindole, barbituric acid, and 1-(3-chlorophenyl)-3-methyl-2-pyrazolin-5-one) (1.2 mmol) on irradiating in a microwave oven gave solid products which were washed with diethyl ether to give pure products **2**−**7**.

*Synthesis of 3-(4-Hydroxy-3,5-dimethoxybenzylidene)-1,3-dihydroindol-2-one (**2**).* A finely ground mixture of syringaldehyde (100 mg, 1 mmol) and oxindole (84.34 mg, 1.2 mmol) was irradiated in a microwave oven for 1 min. The completion of the reaction was checked by TLC. The solid mass was washed with diethyl ether to give pure product **2**. Yield 80%. Yellow solid. Mp 200 °C. ν_{max} (KBr, cm^{-1}): 3401 (NH), 3205 (OH), 1598 (C═O). ^1H NMR (300 MHz, DMSO-d_6, δ) 3.79 (s, 3H, OCH_3), 3.82 (s, 3H, OCH_3), 6.80−6.98 (m, 2H, ArH), 7.05 (s, 1H, ArH), 7.13−7.22 (m, 1H, ArH), 7.54−7.82 (m, 2H, ArH), 8.07 (s, 1H, ═CH), 9.16, 9.30 (NH, D_2O exchange), 10.53 (OH, D_2O exchange). ^{13}C NMR (normal/DEPT-135) ($CDCl_3$, δ) 56.4 (+ve, OCH_3), 109.3 (+ve, CH), 109.9 (+ve, CH), 110.1 (+ve, CH), 118.7 (+ve, CH), 121.6 (C), 121.9 (+ve, CH), 122.8 (C), 125.8 (+ve, CH), 128.1 (C), 129.5 (C), 136.5 (C), 138.2 (+ve, CH), 138.6 (C), 141.2 (C), 146.5 (C), 170.1 (C═O). MS (FAB) 298 (M^+ + 1). Anal. Calcd for $C_{17}H_{15}NO_4$: C, 68.68; H, 5.09; N, 4.71. Found: C, 68.69, H, 5.08, N, 4.79.

*Synthesis of 1-(2,6-Dichlorophenyl)-3-(4-hydroxy-3,5-dimethoxybenzylidene)-1,3-dihydroindol-2-one (**3**).* A finely ground mixture of syringaldehyde (100 mg, 1 mmol) and indolinone (84.34 mg, 1.2 mmol) was irradiated in a microwave oven for 1 min. The completion of reaction was checked by TLC. The solid mass was washed with diethyl ether to give pure product **3**. Yield 82%. Yellow solid. Mp 150 °C. ν_{max} (KBr, cm^{-1}): 3215 (OH), 1612 (C═O). ^1H NMR (300 MHz, DMSO-d_6, δ) 3.81 (s, 3H, OCH_3), 3.82 (s, 3H, OCH_3), 6.39−6.46 (m, 1H, ArH), 7.08−7.24 (m, 3H, ArH), 7.62 (t, *J* = 8.1 Hz,1H, ArH), 7.76 (d, *J* = 8.7 Hz, 1H, ArH), 7.78−7.99 (m, 2H, ArH), 7.99−8.06 (m, 2H, ArH), 9.76 (OH, D_2O exchange). ^{13}C NMR (normal/DEPT-135) ($CDCl_3$, δ) 56.5 (+ve, OCH_3), 106.7 (+ve, CH), 108.7 (+ve, CH), 109.3 (+ve, CH), 118.7 (+ve, CH), 122.4 (+ve, CH), 124.6 (C), 125.8 (C), 128.4 (+ve, CH), 129.4 (+ve, CH), 130.6 (+ve, CH), 135.7 (C), 136.7 (C), 138.1 (C), 139.1 (+ve, CH), 142.1 (C), 146.6 (C), 167.2 (C═O). MS (FAB) 441 (M^+ + 1). Anal. Calcd for $C_{23}H_{15}Cl_2NO_4$: C, 62.46; H, 3.87; N, 3.17. Found: C, 62.49; H, 3.88; N, 3.19.

*Synthesis of (4Z)-4-(4-Hydroxy-3,5-dimethoxybenzylidene)-1-(3-chlorophenyl)-3-methyl-1H-pyrazol-5(4H)-one (**4**).* A finely ground mixture of syringaldehyde (100 mg, 1 mmol) and 1-(3-chlorophenyl)-3-methyl-2-pyrazolin-5-one (137 mg, 1.2 mmol) was irradiated in a microwave oven for 1 min. The completion of reaction was checked by TLC. The solid mass was washed with diethyl ether to give pure product **4**. Yield: 81%. Mp 184 °C. ν_{max} (KBr)/cm^{-1} 3205 (OH), 1598 (C═O). ^1H NMR (300 MHz, DMSO-d_6, δ) 2.31 (s, 3H, CH_3), 3.82 (s, 3H, OCH_3), 3.86 (s, 3H, OCH_3), 7.19 (s, 2H, ArH), 7.45 (t, 1H, *J* = 8.1 Hz, ArH),7.73 (s, 1H, ArH), 7.92 (d, *J* = 8.4 Hz, 1H, ArH), 8.07 (s, 1H, ArH), 8.24 (s, 1H, ═CH), 9.76 (OH, D_2O exchange). ^{13}C NMR (normal/DEPT-135, δ) 33.6 (CH_3), 56.2 (OCH_3), 56.3 (OCH_3), 104.6 (CH), 112.1 (CH), 116.6 (CH), 118.4 (CH), 120.2 (C), 124.1 (CH), 125.1 (C), 129.6 (CH), 129.7 (CH), 132.1 (C), 133.6 (C), 134 (C), 139.5 (C), 147 (C), 147.3 (C), 148.3 (CH), 151.4 (C). MS (FAB) 373 (M + 1). Anal. Calcd for $C_{19}H_{17}N_2O_4$: C, 61.21; H, 4.60; N, 7.51. Found: C, 61.19; H, 4.61; N, 7.49.

*Synthesis of 5-(4-Hydroxy-3,5-dimethoxybenzylidene)-1,3-dimethylpyrimidine-2,4,6-(1H,3H,5H)-trione (**5**).* A finely ground mixture of syringaldehyde (100 mg, 1 mmol) and 1,3-dimethylbarbituric acid (103 mg, 1.2 mmol) was irradiated in a microwave oven for 1 min. The completion of reaction was checked by TLC. The solid mass was washed with diethyl ether to give pure product **5**. Yield: 95%. Mp 237 °C. ν_{max} (KBr)/cm^{-1} 3425(OH), 1656 (C═O). ^1H NMR (300 MHz, DMSO-d_6, δ) 3.22 (s, 6H, 2× CH_3), 3.83 (s, 6H, 2 × OCH_3), 7.97 (s, 2H, ArH), 8.31 (s, 1H, ═CH), 10.03 (OH, D_2O exchange). ^{13}C NMR (normal/DEPT-135, δ) 24.5 (CH_3), 32.4 (CH_3), 54.4 (2 × OCH_3), 111.9 (CH), 112.2 (CH), 141.3 (C), 145.4 (C), 149.3 (C═O), 156.2 (C═O). MS (FAB) 321 (M + 1). Anal. Calcd for $C_{15}H_{16}N_2O_6$: C, 56.25; H, 5.04; N, 8.75. Found: C, 56.28; H, 5.01; N, 8.76.

*Synthesis of 4-(5-Bromo-1H-indol-3-ylmethylene)-2-(3-chlorophenyl)-5-methyl-2,4-dihydropyrazol-3-one (**6**).* A finely ground mixture of 5-bromoindole-3-carboxaldehyde (100 mg, 1 mmol) and 1-(3-chlorophenyl)-3-methyl-2-pyrazolin-5-one (137 mg, 1.2 mmol) was irradiated in a microwave oven for 1 min. The completion of reaction was checked by TLC. The solid mass was washed with diethyl ether to give pure product **6**. Orange solid. Yield 65%. Mp >240 °C. ^1H NMR (300 MHz, DMSO-d_6, δ) 2.40 (s, 3H, CH_3), 7.20 (d, *J* = 9.0 Hz, 1H, ArH), 7.43 (t, *J* = 9.0 Hz, 2H, ArH), 7.53 (d, *J* = 8.4 Hz, 1H, ArH), 7.94 (d, *J* = 8.1 Hz, 1H, ArH), 8.13 (d, *J* = 9.0 Hz, 2H, ArH), 8.49 (s, 1H, ═CH), 9.70 (s, 1H, indole2-H), 12.7 (NH, D_2O exchange). ^{13}C NMR (normal/DEPT-135) (DMSO + $CDCl_3$, δ) 13.02 (+ve, CH_3), 111.779 (C), 114.507 (+ve, CH), 115.142 (C), 115.81 (+ve, CH), 117.19 (+ve, CH), 118.61 (C), 121.23 (+ve, CH), 123.22 (+ve, CH), 125.86 (+ve, CH), 129.96 (+ve, CH), 133.29 (C), 135.13 (C), 137.29 (+ve, CH), 139.02 (+ve, CH), 139.93 (C), 151.43 (C), 162.85 (C). Anal. Calcd for $C_{19}H_{13}BrClN_3O$: C, 55.03; H, 3.16; N, 10.13. Found: C, 54.64; H, 3.19; N, 11.68.

*Synthesis of (Z)-1-(2,6-Dichlorophenyl)-3-((pyridin-2-yl)methylene)indolin-2-one (**7**).* A finely ground mixture of pyridine-2-carboxaldehyde (100 mg, 1 mmol) and indolinone (137 mg, 1.2 mmol) was irradiated in a microwave oven for 1 min. The completion of reaction was checked by TLC. The solid mass was washed with diethyl ether to give pure product **7**. Shiny yellow solid. Yield 86%. Mp 188 °C. ν_{max} (KBr): 1668 (C═O). ^1H NMR (300 MHz, DMSO-d_6, δ) 6.45 (d, *J* = 7.8 Hz, 1H, ArH), 7.16 (t, *J* = 7.5 Hz, 1H, ArH), 7.33 (t, *J* = 7.5 Hz, 1H, ArH), 7.50−7.54 (m, 1H, ArH), 7.65 (d, *J* = 7.8 Hz, 1H, ArH), 7.78 (d, *J* = 8.4 Hz, 3H, ArH), 7.98 (s, 2H, ArH), 8.94 (d, *J* = 7.5 Hz, 1H, ArH). 9.22 (d, *J* = 7.5 Hz, 1H, ArH). ^{13}C NMR (normal/DEPT-135) ($CDCl_3$, δ) 109.2 (+ve, CH), 122.4 (+ve, CH), 123.2 (+ve, CH), 123.7 (+ve, CH), 124.4 (C), 127.7 (+ve, CH), 128.8 (+ve, CH), 128.91 (+ve, CH), 128.94 (+ve, CH), 129.7 (+ve, CH), 130.6 (+ve, CH), 135.71 (C), 135.73 (C), 135.9 (C), 136.9 (+ve, CH), 141.5 (C), 144.8 (+ve, CH), 167.1(C). FAB mass *m*/*z* 366 (M^+)

dx.doi.org/10.1021/jm300644g | J. Med. Chem. 2012, 55, 6381−6390

366:368:370 (9:6:1). Anal. Calcd for $C_{20}H_{12}Cl_2N_2O$: C, 65.41; H, 3.29; N, 7.63. Found: C, 65.15; H, 3.28; N, 7.38.

*General Procedure for the Synthesis of Compounds **11** and **12**.* An equimolar mixture of indole-3-carboxaldehyde and epichlorohydrin was stirred in CH_3CN in the presence of NaH to give N-substituted product **8** which on reaction with 1-(3-chlorophenyl)-3-methyl-2-pyrazolin-5-one and indolinone provided compounds **9** and **10**, respectively. Treatment of compounds **9** and **10** with piperidine under MWI gave compounds **11** and **12**, respectively.

*Synthesis of (4Z)-1-(3-Chlorophenyl)-4-((1-(2-hydroxy-3-(piperidin-1-yl)propyl)-1H-indol-3-yl)methylene)-3-methyl-1H-pyrazol-5(4H)-one (**11**).* Yellow solid. Yield 83%. Mp 148 °C. ν_{max} (KBr): 1694 (C═O). ^{1}H NMR (300 MHz, DMSO-d_6, δ) 1.40−1.56 (m, 7H, 3 × CH_2 + CH), 2.28−2.51 (m, 8H, 2 × CH_2 + CH, CH_3), 4.03−4.51 (m, 3H, CH_2 + CH), 5.15 (br, 1H, OH), 7.22−7.37 (m, 4H, ArH), 7.68 (s, 1H, ArH), 7.96−8.10 (m, 3H, 3ArH), 8.21 (s, 1H, ═CH), 9.84 (s, 1H, indole2-H). ^{13}C NMR (DEPT-135) ($CDCl_3$, δ) 13.6 (+ve, CH_3), 24.4 (−ve, CH_2), 26.4 (−ve, CH_2), 30.1 (−ve, CH_2), 52.0 (−ve, CH_2), 55.0 (−ve, CH_2), 62.0 (−ve, CH_2), 66.4 (+ve, CH), 111.9 (+ve, CH), 112.5 (C), 117.1 (C), 118.3 (+ve, CH), 119.2 (+ve, CH), 119.7 (+ve, CH), 123.0 (C), 124.1 (+ve, CH), 124.5 (+ve, CH), 130.1 (C), 134.8 (C), 136.0 (+ve, CH), 137.8 (C), 140.4 (C), 141.8 (+ve, CH), 151.3 (C), 163.8 (C═O). MS (FAB) 476 (M^+). Anal. Calcd for $C_{27}H_{29}ClN_4O_2$: C, 67.99; H, 6.13; N, 11.75. Found: C, 67.78; H, 6.14; N, 11.76.

*Synthesis of (Z)-1-(2,6-Dichlorophenyl)-3-((1-(2-hydroxy-3-(piperidin-1-yl)propyl)-1H-indol-3-yl)methylene)indolin-2-one (**12**).* Yellow solid. Yield 83%. Mp 181 °C. ν_{max} (KBr): 1694 (C═O). ^{1}H NMR (300 MHz, DMSO-d_6, δ) 1.22−1.47 (m, 6H, 3 × CH_2), 2.20−2.35 (m, 6H, 3 × CH_2), 3.97−4.19 (m, 2H, CH_2), 4.40−4.44 (m, 1H, CH), 5.01 (br, 1H, OH), 6.42 (d, J = 7.5 Hz, 1H ArH), 7.14 (t, 2H, J = 3.6 Hz, ArH), 7.28−7.30 (m, 2H, ArH), 7.59−7.64 (t, J = 7.8 Hz, 2H, ArH), 7.77 (d, J = 7.8 Hz, 2H, ArH), 8.08 (d, J = 5.7 Hz, 1H, ArH), 8.26 (d, J = 4.8 Hz, 1H, ArH), 8.35 (s, 1H, ═CH), 9.42 (s, 1H, indole2-H). ^{13}C NMR (DEPT-135) ($CDCl_3$, δ) 24.0 (−ve, CH_2), 25.8 (−ve, CH_2), 50.2 (−ve, CH_2), 51.3 (−ve, CH_2), 54.5 (−ve, CH_2), 61.5 (−ve, CH_2), 61.8 (−ve, CH_2), 66.0 (+ve, CH), 108.6 (+ve, CH), 110.9 (+ve, CH), 111.7 (+ve, CH), 117.5 (C), 117.8 (+ve, CH), 118.0 (+ve, CH), 120.1 (+ve, CH), 121.5 (+ve, CH), 122.1 (+ve, CH), 122.8 (+ve, CH), 126.7 (+ve, CH), 127.9 (+ve, CH), 128.9 (+ve, CH), 130.4 (C), 131.8 (C), 132.3 (C), 136.0 (C), 136.9 (C), 137.6 (C), 138.8 (C), 163.8 (C═O). MS (FAB) 545 (M^+). Anal. Calcd for $C_{31}H_{29}Cl_2N_3O_2$: C, 68.13; H, 5.35; N, 7.69. Found: C, 68.18; H, 5.34; N, 7.66.

In Vitro Anticancer Screening. Anticancer screening of compounds was carried out at National Cancer Institute, Bethesda, MD, U.S., as per the standard procedure.[23] Human tumor cell lines of the cancer screening panel were grown in RPMI 1640 medium containing 5% fetal bovine serum and 2 mM L-glutamine. Cells were inoculated into 96-well microtiter plates in 100 μL at plating densities ranging from 5000 to 40 000 cells/well depending on the doubling time of individual cell lines. After cell inoculation, the microtiter plates were incubated at 37 °C, 5% CO_2, 95% air, and 100% relative humidity for 24 h prior to addition of experimental drugs. After 24 h, two plates of each cell line were fixed in situ with TCA to represent a measurement of the cell population for each cell line at the time of compound addition (Tz). Compounds were solubilized in dimethyl sulfoxide at 400-fold the desired final maximum test concentration and stored frozen prior to use. At the time of compound addition, an aliquot of frozen concentrate was thawed and diluted to twice the desired final maximum test concentration with complete medium containing 50 μg/mL gentamicin. Additional 4, 10-fold, or $^1/_2$ log serial dilutions were made to provide a total of five compound concentrations plus control. Aliquots of 100 μL of these different drug dilutions were added to the appropriate microtiter well already containing 100 μL of medium, resulting in the required final concentrations. Following compound addition, the plates were incubated for an additional 48 h at 37 °C, 5% CO_2, 95% air, and 100% relative humidity. For adherent cells, the assay was terminated by the addition of cold TCA. Cells were fixed in situ by the gentle addition of 50 μL of cold 50% (w/v) TCA (final concentration, 10% TCA) and incubated for 60 min at 4 °C. The supernatant was discarded, and the plates were washed five times with tap water and air-dried. Sulforhodamine B (SRB) solution (100 μL) at 0.4% (w/v) in 1% acetic acid was added to each well, and plates were incubated for 10 min at room temperature. After staining, unbound dye was removed by washing five times with 1% acetic acid and the plates were air-dried. Bound stain was subsequently solubilized with 10 mM Trizma base, and the absorbance was read on an automated plate reader at a wavelength of 515 nm. By use of the absorbance measurements [time zero (Tz), control growth (C), and test growth in the presence of compound at five concentration levels (Ti)], the percentage growth was calculated at each of the compound concentrations. Percentage growth inhibition was calculated as

$$[(\mathrm{Ti} - \mathrm{Tz})/(C - \mathrm{Tz})] \times 100$$

for concentrations for which Ti ≥ Tz, and

$$[(\mathrm{Ti} - \mathrm{Tz})/\mathrm{Tz}] \times 100$$

for concentrations for which Ti < Tz.

Growth inhibition of 50% (GI_{50}) was calculated from $[(\mathrm{Ti} - \mathrm{Tz})/(C - \mathrm{Tz})] \times 100 = 50$, which was the compound concentration resulting in a 50% reduction in the net protein increase (as measured by SRB staining) in control cells during the drug incubation. The drug concentration resulting in total growth inhibition (TGI) was calculated from Ti = Tz. The LC_{50} (concentration of drug resulting in a 50% reduction in the measured protein at the end of the drug treatment compared to that at the beginning) indicating a net loss of cells following treatment was calculated from $[(\mathrm{Ti} - \mathrm{Tz})/\mathrm{Tz}] \times 100 = -50$. Values were calculated for each of these three parameters if the level of activity was reached; however, if the effect was not reached or exceeded, the value for that parameter was expressed as greater or less than the maximum or minimum concentration tested.

UV−Visible Spectral Studies. UV−vis spectral studies were performed on BioTek PowerWave XS instrument. 10^{-3} M stock solutions of the compounds were prepared in ethanol−HEPES buffer (1:1), pH 7.2. The enzyme stock solution was prepared by diluting 6 μL of dihydrofolate reductase to 1 mL in ethanol−HEPES buffer (1:1), pH 7.2. The spectra were recorded on incremental addition of 10 μL of enzyme stock solution to 10^{-4} M (prepared by diluting stock solution) compound solution.

Equation Used for Calculating Binding Constants: Benesi−Hildebrand Equation.[26] The equation is the following:

$$1/(A_f - A_{obs}) = 1/(A_f - A_{fc}) + \{1/[K(A_f - A_{fc})]\}[\mathrm{ligand}]$$

where K is the binding constant, A_f is the absorbance of the free host, A_{obs} is the absorbance observed, and A_{fc} is the absorbance at saturation.

Dihydrofolate Reductase Inhibition Assay. The dihydrofolate reductase inhibition assay was performed as per the manual of the DHFR assay kit (Sigma product code CS0340). All the dilutions were made in assay buffer, pH 7.5. 10 mM stock solutions of dihydrofolic acid and NADPH in assay buffer were prepared. Stock solutions of the test compounds with different concentrations were prepared in DMSO, and an amount of 20 μL of each was taken to attain final concentration of 10^{-8}, 10^{-7}, 10^{-6}, 10^{-5}, and 10^{-4} M in the respective wells of 96-well plate containing assay buffer. An amount of 0.1 unit of DHFR as supplied in the kit was diluted, and an amount of 20 μL of its 3×10^{-3} unit was used in each reaction. Each well of the 96-well plate was charged with 157.8 μL of assay buffer. Then 1.2 μL of NADPH solution was added to each well except 1A and 1B, and 20 μL of test compound (including methotrexate as positive control) was added to each well except 1A−H. The reaction was started by the addition of 1 μL of dihydrofolic acid to each well except 1C and 1D. 1G and 1H contained 20 μL of DMSO to check any inhibition of enzyme activity due to DMSO. The change in absorbance at 340 nm was monitored as a function of time. Percentage inhibition of enzymatic activity was calculated after nullifying the effects of NADPH, folate, and solvent. IC_{50} was calculated by plotting a graph between percentage inhibition and the corresponding concentration of the compound.

■ ASSOCIATED CONTENT

Supporting Information

^{1}H NMR spectra and UV−vis spectra of pure compounds as well as in combination with DHFR, molecular modeling, and detailed anticancer activities of compounds. This material is available free of charge via the Internet at http://pubs.acs.org.

■ AUTHOR INFORMATION

Corresponding Author

*Phone: 91-183-2258802-09, extension 3495. E-mail: palwinder_singh_2000@yahoo.com.

Notes

The authors declare no competing financial interest.

■ ACKNOWLEDGMENTS

Financial assistance from Council of Scientific and Industrial Research, New Delhi, India, is gratefully acknowledged. M.K. thanks UGC-SAP, and S.S. thanks Guru Nanak Dev University, Amritsar, India, for a fellowship. Thanks are due to NCI, Bethesda, MD, U.S., for anticancer screening of compounds. Fruitful suggestions and comments of the reviewers are gratefully acknowledged. The sincere efforts of Prof. A. S. Brar, Vice-Chancellor, Guru Nanak Dev University, for creating state of the art research facilities are also gratefully acknowledged.

■ ABBREVIATIONS USED

DHFR, dihydrfolate reductase; TMP, trimethoprim; TGI, total growth inhibition; LC_{50}, 50% lethal concentration; GI_{50}, 50% growth inhibition; IC_{50}, 50% inhibitory concentration; TPSA, total polar surface area; HEPES, 4-(2-hydroxyethyl)piperazine-1-ethanesulfonic acid sodium salt; TS, thymidylate synthase; TP, thymidylate phosphorylase; MWI, microwave irradiation; TI, therapeutic index; SRB, sulforhodamine

■ REFERENCES

(1) Groff, J. P. A Structure−Function Study of Dihydrofolate Reductase: The Role of Tryptophan Residues. Ph.D. Thesis, University of Iowa, 1980.

(2) Roth, B. A.; Falco, E. A.; Hitchings, G. H.; Bushby, R. M. 5-Benzyl-2,4-diaminopyrimidines as Antibacterial Agents.1.Synthesis and Antibacterial Activity in Vitro. *J. Med. Pharm. Chem.* **1962**, *5*, 1103−1123.

(3) Carl, W. S.; Michael, E. G.; Charles, A. N. Metabolism of Trimethoprim in Man and Measurement of a New Metabolite: A New Fluorescence Assay. *J. Infect. Dis.* **1973**, *128*, S580−S583.

(4) Heidelberger, C.; Chaudhuri, N. K.; Danneberg, P.; Mooren, D.; Griesbach, L.; Duschinsky, K.; Schnitzer, R.; Pleven, E.; Scheiner, J. Fluorinated Pyrimidines, a New Class of Tumour Inhibitory Compounds. *Nature* **1957**, *179*, 663−666.

(5) Anticancer activity of 5-fluorouracil available in NCI data base (www.dtp.nci.nih.gov), NSC 19893.

(6) Anticancer activity of methotrexate available in NCI data base (www.dtp.nci.nih.gov), NSC 740.

(7) Chabner, B. A. Methotrexate. In *Clinical Pharmacology of Antineoplastic Agents*; Chabner, B. A., Ed.; W. B. Saunders: Philadelphia, PA, 1982.

(8) Jolivet, J.; Schilsky, R. L.; Bailey, B. D.; Drake, J. C.; Chabner, B. A. Synthesis, Retention and Biological Activity of Methotrexate Polyglutamates in Cultured Human Breast Cancer Cells. *J. Clin. Invest.* **1982**, *70*, 351−360.

(9) Li, R.; Sirawaraporn, R.; Chitnumsub, P.; Sirawaraporn, W.; Wooden, J.; Athappilly, F.; Turley, S.; Hol, W. G. J. Three-Dimensional Structure of *M. tuberculosis* Dihydrofolate Reductase Reveals Opportunities for the Design of Novel Tuberculosis Drugs. *J. Mol. Biol.* **2000**, *295*, 307−323.

(10) Oefner, C.; Bandera, M.; Haldimann, A.; Laue, H.; Schulz, H.; Mukhija, S.; Parisi, S.; Weiss, L.; Lociuro, S.; Dale, G. E. Increased Hydrophobic Interactions of Iclaprim with *Staphylococcus aureus* Dihydrofolate Reductase Are Responsible for the Increase in Affinity and Antibacterial Activity. *J. Antimicrob. Chemother.* **2009**, *63*, 687−698.

(11) Heaslet, H.; Harris, M.; Fahnoe, K.; Sarver, R.; Putz, H.; Chang, J.; Subramanyam, C.; Barreiro, G.; Miller, J. R. Structural Comparison of Chromosomal and Exogenous Dihydrofolate Reductase from *Staphylococcus aureus* in Complex with the Potent Inhibitor Trimethoprim. *Proteins* **2009**, *76*, 706−717.

(12) Donkor, I. O.; Li, H.; Queener, S. F. Synthesis and DHFR Inhibitory Activity of a Series of 6-Substituted-2,4-diaminothieno[2,3-*d*]pyrimidines. *Eur. J. Med. Chem.* **2003**, *38*, 605−611.

(13) Gangjee, A.; Vidwans, A.; Elzein, E.; McGuire, J. J.; Queener, S. F.; Kisliuk, R. L. Synthesis, Antifolate and Antitumour Activities of Classical and Nonclassical 2-Amino-4-oxo-5-substituted-pyrrolo[2,3-*d*]pyrimidines. *J. Med. Chem.* **2001**, *44*, 1993−2003.

(14) Wyss, P. C.; Gerber, P.; Hartman, P. G.; Hubschwerlen, C.; Locher, H.; Marty, H. P.; Stahl, M. Novel Dihydrofolate Reductase Inhibitors. Structure-Based versus Diversity-Based Library Design and High-Throughput Synthesis and Screening. *J. Med. Chem.* **2003**, *46*, 2304−2312.

(15) Gangjee, A.; Qiu, Y.; Li, W.; Kisliuk, R. L. Potent Dual Thymidylate Synthase and Dihydrofolate Reductase Inhibitors: Classical and Nonclasssical 2-Amino-4-oxo-5-arylthio-substituted-6-methylthieno[2,3-*d*]pyrimidine Antifolates. *J. Med. Chem.* **2008**, *51*, 5789−5797.

(16) Rosowsky, A.; Fu, H.; Chan, D. C. M.; Queener, S. F. Synthesis of 2,4-Diamino-6-[2′-*O*-(ω-carboxyalkyl)oxydibenz[*b*,*f*]azepin-5-yl]-methylpteridines as Potent and Selective Inhibitors of *Pneumocystis carnii*, *Toxoplasma gondii*, and *Mycobacterium avium* Dihydrofolate Reductase. *J. Med. Chem.* **2004**, *47*, 2475−2485.

(17) Gangjee, A.; Li, W.; Kisliuk, R.; Cody, V.; Pace, J.; Piraino, J.; Makin, J. Design, Synthesis and X-ray Crystal Structure of Classical and Nonclassical 2-Amino-4-oxo-5-substituted-pyrrolo[2,3-*d*]-pyrimidines as Dual Thymidylate Synthase and Dihydrofolate Reductase Inhibitors and as Potential Antitumour Agents. *J. Med. Chem.* **2009**, *52*, 4892−4902.

(18) Li, X.; Hilgers, M.; Cunningham, M.; Chen, Z.; Trzoss, M.; Zhang, J.; Kohnen, L.; Lam, T.; Creighton, C.; Kedar, G. C.; Nelson, K.; Kwan, B.; Stidham, M.; Brown-Driver, M.; Shaw, K. J.; Finn, J. Structure Based Design of New DHFR-Based Antibacterial Agents: 7-Aryl-2,4-diaminoquinazolines. *Bioorg. Med. Chem. Lett.* **2011**, *21*, 5171−5176.

(19) Schneider, P.; Hawser, S.; Islam, K. Iclaprim, a Novel Diamino Pyrimidine with Potant Activity on Trimethoprim Sensitive and Resistant Bacteria. *Bioorg. Med. Chem. Lett.* **2003**, *13*, 4217−4221.

(20) Rees, R. W. A.; Chai, S. Y.; Winkley, M. W.; Russel, P. B. Antimalarial Activity of Some Novel Derivatives of 2,4-Diamino-(5-*p*-chlorophenyl)-6-ethylpyrimidine (Pyrimethamine). *J. Med. Chem.* **1976**, *19* (5), 723−725.

(21) Then, R. L.; Hermann, F. Properties of Brodimoprim as an Inhibitor of Dihydrofolate Reductases. *Chemotherapy* **1984**, *30* (1), 18−25.

(22) Lai, W. G.; Zahid, N.; Uetrecht, J. P. Metabolism of Trimethoprim to a Reactive Iminioquinone Methide by Activated Human Neutrophils and Hepatic Microsomes. *J. Pharmacol. Expt. Ther* **1999**, *291*, 292−299.

(23) Developmental Therapeutics Program, NCI/NIH. www.dtp.nci.nih.gov.

(24) Anticancer activity of indomethacin available in NCI data base (www.dtp.nci.nih.gov), NSC 77541.

(25) Available from NCI data base (www.dtp.nci.nih.gov), NSC 106568. Trimethoprim did not show tumor growth inhibition at 10^{-5} M.

(26) Hildebrand, J. H.; Benesi, H. A. A Spectrophotometric Investigation of the Interaction of Iodine with Aromatic Hydrocarbons. *J. Am. Chem. Soc.* **1949**, *71*, 2703−2707.